

Article

Evaluation of Different Irrigation Methods for an Apple Orchard Using an Aerial Imaging System

Duke M. Bulanon ^{1,*}, John Lonai ¹, Heather Skovgard ¹ and Esmaeil Fallahi ²

¹ Department of Physics and Engineering, Northwest Nazarene University, Nampa 83686, USA; jlonai@nnu.edu (J.L.); hskovgard@nnu.edu (H.S.)

² Parma Research and Extension Center, University of Idaho, Parma 83660, USA; efallahi@uidaho.edu

* Correspondence: dbulanon@nnu.edu; Tel.: +1-208-467-8047

Academic Editors: Gonzalo Pajares Martinsanz and Wolfgang Kainz

Received: 9 April 2016; Accepted: 26 May 2016; Published: 1 June 2016

Abstract: Regular monitoring and assessment of crops is one of the keys to optimal crop production. This research presents the development of a monitoring system called the Crop Monitoring and Assessment Platform (C-MAP). The C-MAP is composed of an image acquisition unit which is an off-the-shelf unmanned aerial vehicle (UAV) equipped with a multispectral camera (near-infrared, green, blue), and an image processing and analysis component. The experimental apple orchard at the Parma Research and Extension Center of the University of Idaho was used as the target for monitoring and evaluation. Five experimental rows of the orchard were randomly treated with five different irrigation methods. An image processing algorithm to detect individual trees was developed to facilitate the analysis of the rows and it was able to detect over 90% of the trees. The image analysis of the experimental rows was based on vegetation indices and results showed that there was a significant difference in the Enhanced Normalized Difference Vegetation Index (ENDVI) among the five different irrigation methods. This demonstrates that the C-MAP has very good potential as a monitoring tool for orchard management.

Keywords: apple; digital image processing; machine vision; unmanned aerial vehicle (UAV); vegetation indices

1. Introduction

In spite of the challenging economic situation of the nation, the specialty crop industry in Idaho is thriving. According to the US Census Bureau, the US population is projected to grow 34% by the year 2060 [1]. With an increasing population, the need to improve production and management of agricultural products has become a necessity [2]. Providing farmers with inexpensive cutting-edge technologies that can assist them in managing their crops will help them run their business more efficiently and make Idaho specialty crops more competitive in the market. Efficiency in the use of crop inputs such as water, chemicals and fertilizers means that fewer of these inputs will be used based upon crop requirements. The benefits of this efficiency will be both economical and environmental.

Remote sensing [3,4] is one of the technologies that has been gaining considerable interest in monitoring row crops. Remote sensing data provide farmers with the ability to monitor crop health and conditions. For example, chlorophyll in the plant reflects green while absorbing the red and blue wavelengths. Stress in plants means higher yellow-red reflectance due to lower chlorophyll content and pigmentation [5]. On the other hand, structural collapse of a dying cell caused by a disease infection has a lower near-infrared (NIR) reflectance [6]. In addition, reflectance in the NIR band has been correlated with applied nitrogen in the field.

Typically in remote sensing [7], data is acquired using manned aircraft mounted with a color-infrared camera and satellite-based imaging [8]. This system is not widely used by farmers as it

is expensive, has low spatial resolution (which means less accuracy), and has low sampling frequency. Although these systems could facilitate in the decision-making of the farmers in crop management, it is not economically feasible for specialty crop application in Idaho. A cost-effective platform is critical for the development of remote sensing for specialty crops.

This paper shows the development of a remote sensing platform, called the Crop Monitoring and Assessment Platform (C-MAP), to support localized specialty crop monitoring needs in Idaho. The C-MAP provides the farmer with an inexpensive, efficient, rapid, and non-invasive field monitoring system on demand.

The C-MAP as a whole is composed of a low-cost unmanned aerial vehicle (UAV) with the sensor module attached. The sensor is modular so it could also be mounted on another mobile platform, e.g., tractor. It will be a remote sensing system that acquires data at a distance; however, unlike remote sensing technologies, e.g., satellite imaging and general aviation aircraft, crop data will be acquired at low altitude and near field features of interest. The C-MAP will be a practical substitute for these expensive remote sensing technologies and is immediately accessible to farmers.

Specifically, this research has the following objectives:

1. To acquire remote sensing data (multispectral images) of apple groves with controlled input of irrigation (water);
2. To use image processing techniques to process the images and analyze the data using vegetation indices (VI).

2. Materials and Methods

2.1. Target Orchards

The target orchard is an experimental apple orchard located at the University of Idaho Parma Research and Extension Center in Parma, Idaho, which is located in the southwest portion of the state of Idaho (Figure 1). The experimental apple orchard was established in the spring and summer of 2002. “Autumn Rose Fuji” trees on RN 29 (Nic 29) rootstock (Columbia Basin Nursery, Quincy WA, USA) were planted at 1.52 m × 4.27 m spacing with an east-west row orientation. “Snow Drift” crab apple on RN 29 rootstock (C & O Nursery, Wenatchee, WA, USA) was planted in each row as a pollinizer between every 10 “Autumn Rose Fuji” trees. The experimental site has a semi-arid climate, with an annual precipitation of about 297 mm and a sandy loam soil. Crested wheatgrass (*Agropyron cristatum* (L.) Gaertn.), which is a drought tolerant grass, was planted as the orchard floor cover in all treatments.

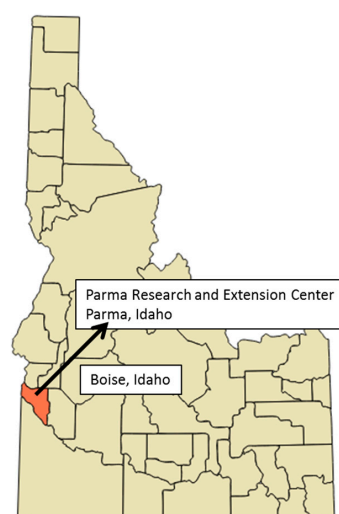


Figure 1. Study area map of experimental orchard.

Five different water delivery methods for apple production were compared in this study: (a) full sprinkler; (b) 50% deficit sprinkler; (c) 50% deficit drip; (d) full drip; and (e) 65% drip. Five experimental rows in the orchard were chosen to be the controlled rows. Figure 2 shows the target orchard and the five controlled rows. Each row was divided into five groups, corresponding to the watering method, and each group was composed of about six to eight trees as shown in Table 1. These different watering methods are management strategies that focus on maximizing yield production. In order to isolate the controlled rows, guard trees were planted between the groups. Their main purpose is to serve as a physical barrier between the groups, so the data obtained from each group is reliable.



Figure 2. Target orchard showing the five experimental rows.

Table 1. Distribution of irrigation methods for the experimental rows.

Tree Groups	Row 1	Row 2	Row 3	Row 4	Row 5
A	Full Sprinkler	50% Deficit Sprinkler	Full Drip	65% Deficit Drip	50% Deficit Drip
B	65% Deficit Drip	50% Deficit Drip	50% Deficit Sprinkler	Full Drip	Full Sprinkler
C	Full Drip	Full Sprinkler	65% Deficit Drip	50% Deficit Drip	50% Deficit Sprinkler
D	50% Deficit Drip	Full Drip	Full Sprinkler	50% Deficit Sprinkler	65% Deficit Drip
E	50% Deficit Sprinkler	65% Deficit Drip	50% Deficit Drip	Full Sprinkler	Full Drip

2.2. Unmanned Aerial System

The unmanned aerial vehicle (UAV) used in this study is the Mikrokopter OktokopterXL, an eight-rotor platform [9]. The UAV has flight and navigation controller that allows both remote control navigation and GPS waypoint navigation. A ground station composed mainly of a personal computer with a receiver provides flight information of the UAV such as altitude, battery level, position, etc. The payload capacity of the UAV is about one kilogram, which allows the UAV to be equipped with an image acquisition system. Figure 3 shows the UAV with its components and Figure 4 shows the UAV over the experimental orchard. The system used in this study is similar to others that have conducted research using multi-rotor UAVs [10–12].



Figure 3. Unmanned aerial vehicle with multispectral camera (vegetation stress camera).



Figure 4. Unmanned aerial vehicle acquiring images over experimental orchard.

2.3. Image Acquisition System

The image acquisition system is a three-band multispectral camera (Figure 2). The multispectral camera is a Canon PowerShot SX280 with 12.1 megapixels, a complementary metal-oxide semiconductor (CMOS) sensor, and a 25 mm wide-angle lens. The filter of the camera was modified to allow it to capture the blue and green wavelengths for the visible band and a short-wave near-infrared (NIR) bandwidth centered at 750 nm. The multispectral camera has first person video capability that allows viewing of video from the ground as well as manual image acquisition. In addition to the multispectral camera, a GoPro camera was also attached to the UAV to collect color video data.

2.4. Image Acquisition

Image acquisition started on 15 May 2013, and ended on 14 July 2013. Images were collected every week and it took place mostly in the morning times between 9 a.m. and 12 p.m. The conditions of the day varied a little over the weeks, but most of the data was taken under clear skies.

For image acquisition using the UAV, the MikroKopter Tool was used to set up the flight. The MikroKopter Tool is a Windows program that allows the operator to adjust the settings of the UAV such as the flight control module and the navigation control module. Figure 5 shows an image of the MikroKopter On-Screen-Display that allows the planning of the waypoint flight for image acquisition. The On-Screen-Display also shows telemetry data such as altitude, speed, location, and battery level. There were two methods for image acquisition: (1) a single waypoint was selected on the middle of the field, and the altitude was set to 100 m. At that altitude the camera was able to take images of the entire field, approximately 7000 m², in a single shot. (2) Several waypoints were inserted on chosen areas so the UAV, at 50 m high, could acquire images that after mosaicking would recreate a single high resolution image of the entire orchard. Figure 6 shows a sample multispectral image of the target orchard.

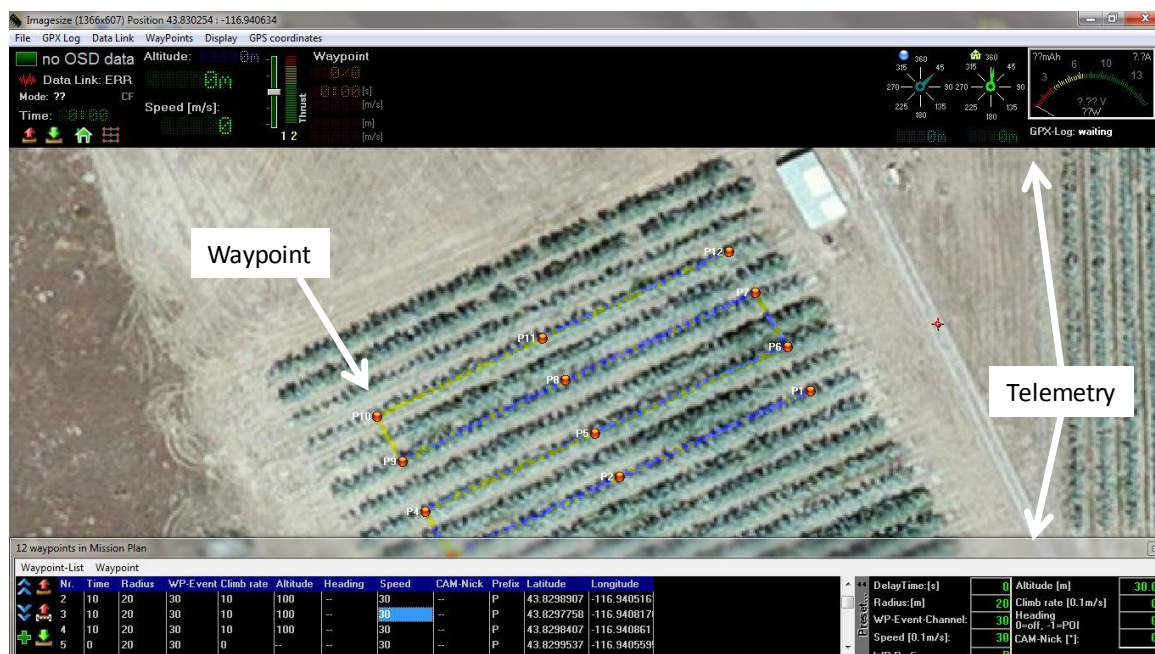


Figure 5. MikroKopter Tool On-Screen-Display for waypoint planning.

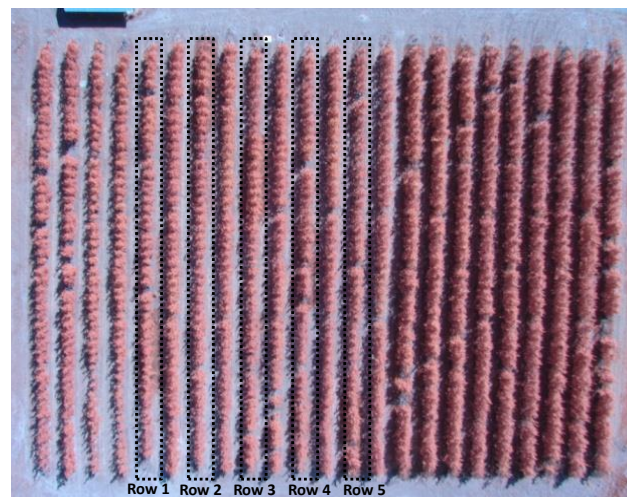


Figure 6. Sample multispectral image of the target orchard.

2.5. Data Analysis

Figure 7 shows the flowchart of the overall methodology of this paper. It starts with image acquisition and is followed by image preprocessing. The image preprocessing is separating the image into three bands. The acquired multispectral image is composed of the following three bands: short-wave NIR, green (G), and blue (B). The tree rows are segmented from the ground using the NIR band and then an image processing algorithm was developed to identify individual trees in each experimental row. The tree identification was based on the watershed algorithm [13,14], a segmentation method for separating connected blobs. Using the segmented trees as an image mask and the three bands, the images were analyzed using the vegetation indices (VI) shown in Table 2. Zakaluk and Ranjan [15] also used similar VI to analyze RGB images of potato plants. Then, the VI were calculated from the pixels of the individual trees from the five experimental rows. The canopy area of each tree (in pixels) was also calculated. Matlab and the Digital Image Processing toolbox were used for image processing and analysis.

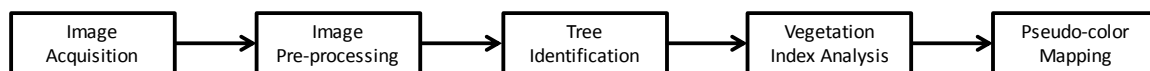


Figure 7. Image acquisition and processing flowchart.

Table 2. Vegetation indices for image analysis.

Vegetation Index	Equation
(1) Green Ratio (GR)	$GR = \frac{G}{NIR}$
(2) Enhanced Normalized Difference Vegetation Index (ENDVI)	$ENDVI = \frac{NIR+G-2(B)}{NIR+G+2(B)}$
(3) Intensity (I)	$I = NIR + G + B$
(4) Normalized Difference Green Near Infrared Index (NDGNI)	$NDGNI = \frac{NIR-G}{NIR+G}$
(5) Saturation (S)	$S = \frac{I-3(B)}{I}$

3. Results and Discussion

3.1. Individual Tree Identification

An image processing algorithm was developed to identify individual trees and facilitate the analysis of the vegetation indices of the five irrigation methods. The algorithm starts with identifying

the individual rows (Figure 8). The row is then segmented and the canopy concavity of the tree is detected. Based on the shape of the tree, the regional maxima is identified and then the result is used to divide the row. The data from the row division and the concavity detection are used as inputs to the watershed algorithm to identify individual markers and separate the individual trees. In this example, 45 out of 49 trees were identified. Results from the other experimental rows showed that over 90% of the trees were recognized. The average vegetation index of the individual trees was then calculated using the tree identification result as an image mask.

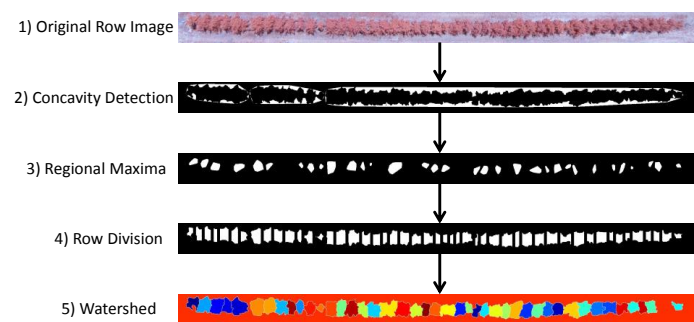


Figure 8. Image processing algorithm for tree identification.

3.2. Vegetation Index Analysis

The five vegetation indices of each tree were calculated. Figure 9 shows the relationship between the averages of the vegetation indices with respect to the irrigation method. These vegetation indices are similar to some of the vegetation indices used for predicting the leaf water potential of potato plants [15] using only RGB. The green ratio index (Figure 9b) shows that Full Drip has the highest value as compared with the other irrigation methods, followed by Full Sprinkler, 65% Drip, 50% Drip, and 50% Sprinkler. Although there is no significant difference between the 65% Drip, Full Sprinkler, and 50% Drip, there is a significant difference between the Full Drip system and the 50% Sprinkler, which shows that the green ratio has a potential to show an anomaly in the field in terms of water input. This could be attributed to the fact that chlorophyll reflects green and absorbs blue and red bands. The green band also has a linear association with nitrogen. The intensity index (Figure 9c) shows differences in index values; however, it did not demonstrate a relationship with the different irrigation methods. As compared to the green ratio index, the ENDVI (Figure 9a) shows a similar trend with the Full Drip having the highest index value and the 50% Sprinkler having the lowest. A statistical analysis conducted on the ENDVI values showed that there is significant difference between the Full Drip and the 65% Drip and the 50% Drip. The Full Drip has a higher ENDVI value as compared with the Full Sprinkler but is not significantly different. As compared to the green ratio equation, the ENDVI amplifies the chlorophyll reflection by adding both the NIR and green bands and subtracting the blue band. Healthier plants reflect higher green and NIR. When a plant is stressed, reflectance of NIR is significantly decreased. A study conducted by Fallahi [16] showed that water stress symptoms were observed in the ground for water deficient trees. They also demonstrated that the drip system has a significantly lower consumption than the sprinkler system. This means that the ENDVI is more sensitive to the changes in water input as compared with the green ratio. A false color image using the ENDVI (Figure 10) was generated with the values of ENDVI ranging from 0 to 1. A high value of ENDVI indicates a higher input of water. The ENDVI false color image clearly shows the variability within the experimental rows, which could provide a hint to a farmer that there is an anomaly in the field, in this case the water input. It can be observed that the portions with high water input (Full Drip and Full Sprinkler) have higher ENDVI values and that the tree groups with water deficit have lower ENDVI values. On the other hand, the NDGNI follows the same pattern as the green ratio index and only shows a significant difference between Full Drip and 50% Sprinkler. The saturation index shows a different pattern where the 50% Sprinkler has the highest index value and the Full Drip has the

lowest index value. It is interesting to note that the saturation index has the same numerator as the ENDVI. Future work will involve the study of these vegetation indices with respect to material input such as nitrogen.

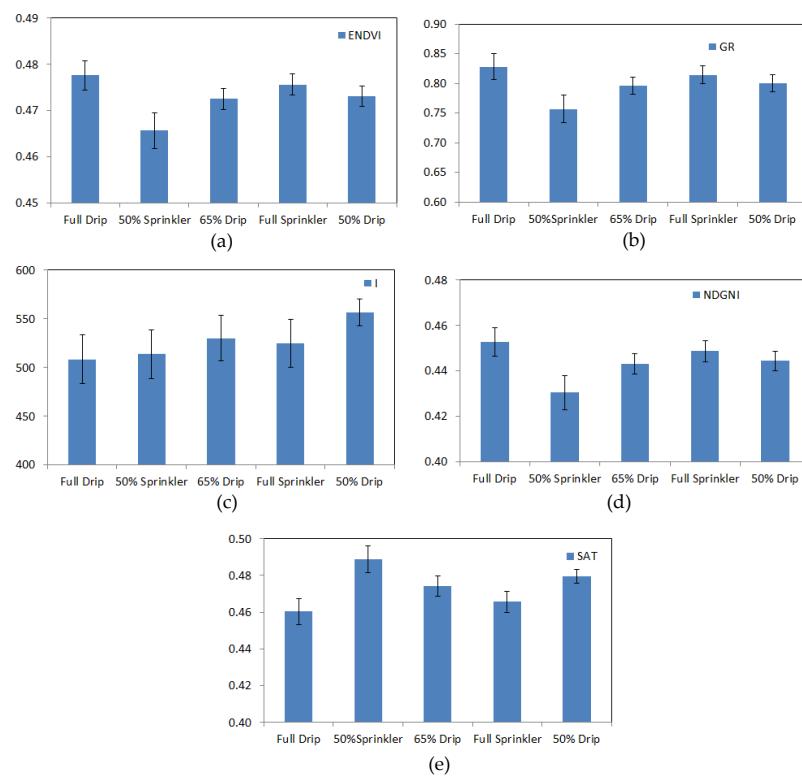


Figure 9. Average vegetation indices of the different irrigation methods: (a) ENDVI; (b) GR; (c) I; (d) NDGNI; (e) SAT.

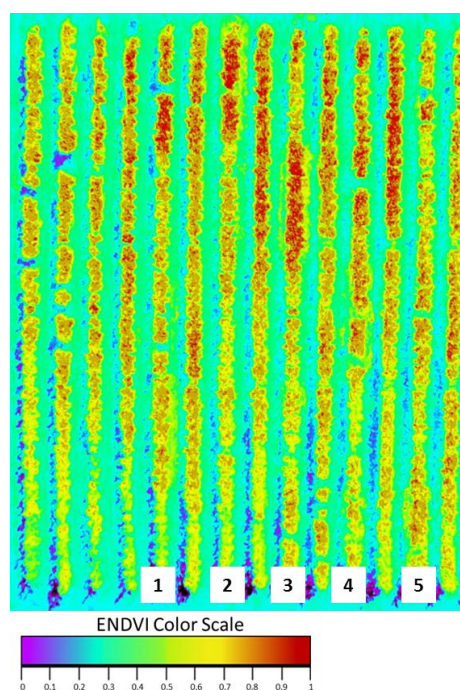


Figure 10. False color image of the experimental rows using ENDVI.

3.3. Tree Canopy Area Analysis

The tree canopy area for each tree was determined by counting the number of pixels for each corresponding blob in the experimental rows. Figure 11 shows that the Full Sprinkler has the highest average area followed by Full Drip, 65% Drip, 50% Drip, and 50% Sprinkler. There is no significant difference between the deficit irrigation methods. This exhibits a good relationship between the canopy area and water input. The difference in tree canopy size can also be observed from the images, even without further processing. These images could be helpful to the farmers because this is difficult to observe on the ground. Ground scouting requires more time and labor. In addition, the result of identifying the canopy area in combination with the vegetation index analysis, such as the ENDVI, can provide farmers with information that would show abnormalities within their field. Future study with canopy area analysis would include the estimation of the leaf area index [10], a common index associated with the physiological process of plants. The C-MAP would be an added tool that farmers could utilize in managing their field.

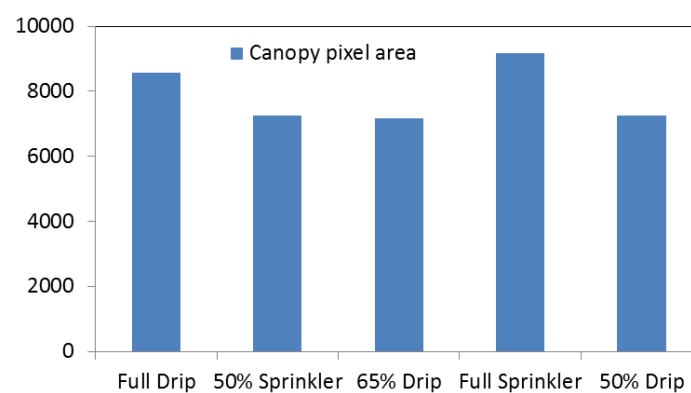


Figure 11. Tree canopy area of the different irrigation methods.

Based on the results from the VI analysis and tree canopy area analysis, the C-MAP has a very high potential for helping farmers in crop management. The advantages of this remote sensing tool over the other alternatives are lower cost, less time needed for field scouting, and less labor resource requirements. With the decreasing cost of small UAVs and computers, the cost of owning this remote sensing platform is within reach for most farmers. This will help farmers in field scouting, which is generally time-consuming and labor-intensive. Replacing field scouting with C-MAP will be economical for farmers. Several UAV companies have also developed very user-friendly applications that work on smart phones and tablets. These applications will help bridge the technological barrier for using this type of technology.

4. Conclusions

A monitoring system (the Crop Monitoring and Assessment Platform) based on a small unmanned aerial system equipped with a multispectral camera was developed. The monitoring system was tested on an experimental apple orchard with five different irrigation methods. The image processing and analysis was based on five vegetation indices; ENDVI, GR, I, NDGNI, and SAT. Results showed that all the vegetation indices except for I show a significant difference between the Full Drip and the 50% Sprinkler systems. Among all the vegetation indices, the ENDVI proved to be a better indicator because it showed a significant difference between Full Drip and the other water deficit methods. A pseudo-color image of the ENDVI demonstrated that it can show abnormalities within the field. This result shows the potential of C-MAP as a monitoring tool to assess orchard variation, and specifically variation in water input. Further tests will be conducted to quantify the correlation between vegetation indices and other material input.

Acknowledgments: This research was supported by the Idaho State Department of Agriculture (Idaho Specialty Crop Block Grant 2012 and 2014), Idaho Space Grant Consortium, and Northwest Nazarene University.

Author Contributions: Duke M. Bulanon conceived the study, made the literature review, designed the experiment, processed the data, interpreted the results and wrote the paper. John Lonai and Heather Skovgard acquired the images, developed the image processing algorithm, and processed the data. Esmail Fallahi designed the target orchard and its treatment, and supervised during the data collection.

Conflicts of Interest: The authors declare no conflict of interest.

Abbreviations

The following abbreviations are used in this manuscript:

B	Blue Band
CMOS	Complementary Metal-Oxide Semiconductor
ENDVI	Enhanced Normalized Difference Vegetation Index
G	Green Band
GR	Green Ratio
I	Intensity
NDGNI	Normalized Difference Green Near Infrared Index
R	Red Band
SAT	Saturation
UAV	Unmanned Aerial Vehicle
VI	Vegetation Index

References

- Colby, S.; Ortman, J.M. Projections of the Size and Composition of the U.S. Population: 2014 to 2060. United States Census Bureau. Available online: <https://www.census.gov/content/dam/Census/library/publications/2015/demo/p25-1143.pdf> (accessed on 4 April 2016).
- Lan, Y.; Thomson, S.J.; Huang, Y.; Hoffmann, W.C.; Zhang, H. Current status and future directions of precision aerial application for site-specific crop management in the USA. *Comput. Electron. Agric.* **2010**, *74*, 34–38. [[CrossRef](#)]
- Lee, W.S.; Alchanatis, V.; Yang, C.; Hirafuji, M.; Moshou, D.; Li, C. Sensing technologies for precision specialty crop production. *Comput. Electron. Agric.* **2010**, *74*, 2–33. [[CrossRef](#)]
- Sugiura, R.; Noguchi, N.; Ishii, K. Remote-sensing technology for vegetation monitoring using an unmanned helicopter. *Biosyst. Eng.* **2005**, *90*, 369–379. [[CrossRef](#)]
- Kondo, N.; Ting, K.C. *Robotics for Bioproduction Systems*; ASAE: St Joseph, MI, USA, 1998.
- Garcia-Ruiz, F.; Sankaran, S.; Maja, J.M.; Lee, W.S.; Rasmussen, J.; Ehsani, R. Comparison of two aerial imaging platforms for identification of Huanglongbing-infected citrus trees. *Comput. Electron. Agric.* **2013**, *91*, 106–115. [[CrossRef](#)]
- Xiang, H.; Tian, L. Development of a low-cost agricultural remote sensing system based on an autonomous unmanned aerial vehicle (UAV). *Biosyst. Eng.* **2011**, *108*, 174–190. [[CrossRef](#)]
- Johnson, A.K.L.; Kinsey-Henderson, A.E. Satellite-based remote sensing for monitoring Baath land use in the sugar industry. *Proc. Aust. Soc. Sugar Cane Technol.* **1997**, *19*, 237–245.
- MikroKopters. Available online: <https://www.mikrokoetter.de/en/home> (accessed on 9 May 2016).
- Corcoles, J.I.; Ortega, J.F.; Hernandez, D.; Moreno, M.A. Estimation of leaf area index in onion (*Allium cepa* L.) using an unmanned aerial vehicle. *Biosyst. Eng.* **2013**, *115*, 31–42. [[CrossRef](#)]
- Capolupo, A.; Kooistra, L.; Berendonk, C.; Boccia, L.; Suomalainen, J. Estimating plant traits of grasslands from UAV-acquired hyperspectral images: A comparison of statistical approaches. *ISPRS Int. J. Geo-Inf.* **2015**, *4*, 2792–2820. [[CrossRef](#)]
- Pajares, G. Overview and current status of remote sensing applications based on Unmanned Aerial Vehicles (UAVs). *Photogramm. Eng. Remote Sens.* **2015**, *81*, 281–329. [[CrossRef](#)]
- Qi, X.; Xing, F.; Foran, D.J.; Yang, L. Robust segmentation of overlapping cells in histopathology specimens using parallel seed detection and repulsive level set. *IEEE Trans. Biomed. Eng.* **2012**, *59*, 754–765. [[PubMed](#)]

14. Bulanon, D.M.; Burks, T.F.; Kim, D.B.; Ritenour, M.A. A Multispectral imaging system for citrus fruit detection. *Environ. Control Biol.* **2010**, *48*, 81–91. [[CrossRef](#)]
15. Zakaluk, R.; Sri Ranjan, R. Predicting the leaf water potential of potato plants using RGB reflectance. *Can. Biosyst. Eng.* **2008**, *50*, 1–7.
16. Fallahi, E.; Fallahi, B.; Shafii, B.; Neilsen, D.; Neilsen, G.H. The impact of long-term evapotranspiration-based water scheduling in various irrigation regismes on tree growth, yield, and fruit quality at Harvest in Fuji Apple. *J. Am. Pomol. Soc.* **2011**, *65*, 42–53.



© 2016 by the authors; licensee MDPI, Basel, Switzerland. This article is an open access article distributed under the terms and conditions of the Creative Commons Attribution (CC-BY) license (<http://creativecommons.org/licenses/by/4.0/>).